FEBS Letters 430 (1998) 12–16 FEBS 20357

Minireview

Measuring elasticity of biological materials by atomic force microscopy

Anja Vinckier[a,b,*], Giorgio Semenza[a,c]

[a] *Department of Biochemistry, Swiss Federal Institute of Technology, ETH Zentrum, Universitätstrasse 16, CH-8092 Zürich, Switzerland*
[b] *Institute of Anatomy, University of Zürich, Winterthurerstrasse 190, CH-8057 Zürich, Switzerland*
[c] *Dipartimento di Chimica e Biochimica Medica, Università di Milano, Via Saldini 50, I-20133 Milan, Italy*

Received 9 May 1998

Abstract Atomic force microscopy (AFM) has proved its value not only for resolving the topographical structure of biological samples, but also for probing inherent properties of biological structures, like local interaction forces, mechanical properties or dynamics in a natural (physiological) environment. This minireview focuses on the acquisition of elasticity data of biomaterials by AFM. A possible theoretical model is presented, followed by a practical 'how to do it with AFM', and, finally, a brief overview of publications in this field is given.

Key words: Atomic force microscopy; Elasticity; Biomaterial; Young's modulus; Resolution

1. Introduction

In the past 12 years, atomic force microscope (AFM), introduced by Binnig et al. [1], has rapidly grown to a valuable and useful tool to look at the topography of materials with a high resolution and to obtain time-dependent dynamic information about biological systems in their natural environment [2–5]. AFM uses a sharp tip at the end of a cantilever, which is scanned in X and Y over a sample mounted on a piezo crystal. Changes in the height (Z direction) due to tip interactions with the substrate are usually optically detected, giving a topographical image of the sample under investigation. Recently, AFM has entered the field of elasticity measurements [6–9]. Up to now, mechanical properties have been studied by several techniques such as optical tweezers [10], rheometry [11], dynamic light scattering [11], fluorescence microscopy [11], the surface force apparatus [12], pipette suction [13], and a number of other techniques ([14–17] and references therein, [18,19]). In AFM, the mechanical properties of biomolecules can be determined accurately and spatially well resolved from force-versus-distance curves, also called force curves [20,21]. In this minireview, a simplified theoretical model to calculate the elasticity of biological samples from force curves will be discussed. Next, a practical description of 'how to do it with AFM' will be presented. Finally, a summary and a list of some publications (Table 1) is given with the focus on 'soft' biological materials.

*Corresponding author (b). Fax: (41) (1) 635 5702.
E-mail: vinckier@anatomie.unizh.ch

Abbreviations: AFM, atomic force microscopy; force curve, force-versus-distance curve; E, Young's modulus or elastic modulus; F, force; Δz, indentation; MTs, microtubules

2. Theory of elasticity

The elasticity of a macroscopic object can be described by Hooke's law in terms of stress and strain [22,23]. Stress is the quantity equal to the deformation force and the strain stands for the amount of deformation. Hooke's law proves that the ratio of the stress to the strain equals a constant depending on the material and the deformation. This constant is the elastic modulus and is specific for the material under investigation. Different kinds of deformations can be distinguished, giving different elastic moduli. We will concentrate on Young's modulus, which is the mechanical resistance of a material while elongating or compressing. Young's modulus – here also called elastic modulus – has as dimensions force per surface area. As long as the stress-strain relation is linear, the deformation of the material is elastic and the material will always regain its original form if no more force is applied. Plasticity of the material shows up in a deviation of the curve from linearity. The material will no longer regain its original form after removal of the external forces. At still higher deformations, the material will break.

This general theory outlined above will be worked out for AFM based on the theory of Hertz [22,24,25] and the mechanics of Sneddon [26]. Using AFM, elasticity measurements are performed by pushing a tip onto the surface of the sample of interest and monitoring force-versus-distance curves. This results in a deformation which is the sum of the deformation of the tip and the deformation of the investigated sample (indentation) under the tip. Although AFM is measured on a microscopic scale, the classical theory is still usable because the tip indents 100 or more atoms of the surface.

The theory of Hertz [22,24,25] describes the deformation, τ, of an elastic sphere under an external load, F, against a rigid flat substrate [27], given by:

$$\tau^3 = \frac{9(1-\mu_{tip}^2)^2 F^2}{16 E_{tip}^2 R} \quad (1)$$

where R is the radius of curvature of the tip and E_{tip} and μ_{tip} are Young's modulus and Poisson's ratio of the tip, respectively. Poisson's ratio is defined as the ratio of the transverse (orthogonal) strain to the strain along the direction of elongation [28]. It is useful for determining how much the material extends orthogonally to the direction in which the force is applied. The value for μ is always between 0 and 0.5 [22,27,29].

The elasticity of the substrate on a microscopic scale can be determined with the force applied to the tip-sample system and the resulting deformation of the sample. The most suitable theory is that of Sneddon which describes an infinitely

PII: S0014-5793(98)00592-4

Table 1
Summary of Young's moduli from several biological samples and commonly used hard substrates

Material	Young's modulus (Pa)	Reference
Glass	50×10^9	[29]
Fused silica	70×10^9	[28]
Au	79×10^9	[27]
Mica	$2–8\times10^{10}$	[30]
Carbon fiber	2.1×10^{11}	[8]
Walls of *Methanospirillum hungatei* GP1	$33–39\times10^9$	[61]
Clathrin cage	$(10\pm1)\times10^6$	unpublished results
Tibial osteons	22.4×10^9	[62]
Cartilage	$0.16–0.6\times10^6$	[29]

Most of these examples are not discussed in the overview.

hard indenter with a special geometry and a flat, deformable substrate [26,27,29,30]. Let's have a closer look to different tip geometries.

2.1. Conical tip

For a conical tip with a semivertical (opening) angle α, the total force F_{cone} as a function of the indentation Δz is described by:

$$F_{cone}(\Delta z) = \frac{2E^*}{\pi(tg(\alpha))}\Delta z^2 \quad (2)$$

where E^* is the relative Young's modulus:

$$\frac{1}{E^*} = \frac{1-\mu_{tip}^2}{E_{tip}} + \frac{1-\mu_{sample}^2}{E_{sample}}. \quad (3)$$

If $E_{sample} \ll E_{tip}$, then $1/E^*$ can be simplified:

$$\frac{1}{E^*} \approx \frac{1-\mu_{sample}^2}{E_{sample}}. \quad (4)$$

E_{sample} is Young's modulus of the studied material and μ_{sample} is the Poisson ratio of the sample.

2.2. Parabolic tip

The force $F_{parabolic}$ as a function of the indentation for a parabolic tip with a radius of curvature R at the apex is:

$$F_{parabolic}(\Delta z) = \frac{4\sqrt{R}}{3}E^*\Delta z^{1.5}. \quad (5)$$

A spherical tip with a radius R also leads to the same formula as Eq. 5, as long as the contact radius $r \leq R$.

The above description assumed deformations arising from perfectly flat elastic substrates; however, some of the following contributions can considerably influence the measured Young's modulus: (1) plastic deformations, (2) the surface energy, and (3) the local shape of a rough surface. For more details, see Heuberger et al. [27]. A more elaborate model can be found in [31,32].

3. 'How to do' the elasticity measurements with AFM [6,7,27,29]

First, a force curve [20,21] has to be recorded on a hard sample as reference (e.g. a glass substrate). Then, the substrate is replaced by the sample of interest and force curves are taken on the soft sample under the same liquid, changing neither the tip nor the position of the laser beam on the cantilever. A typical force curve on a hard sample and on a soft sample is schematically shown in Fig. 1. The difference between the deflection of the cantilever detected on the hard and on the soft samples describes the deformation of the soft sample under the tip load, i.e. how much the tip indents the sample of interest. Plotting the obtained indentation against the force gives force-versus-indentation curves. It is important to use the approaching part of the force curve for calculating the indentation [33] because use of the retracting part leads to wrong measurements of the indentation, due to e.g. adhesive forces.

To determine Young's modulus, force (F)-versus-indentation (Δz) curves are fitted to an equation of the form: $F = a \bullet \Delta z^b$, based on Eq. 2 or Eq. 5. The exponent b depends on the tip shape. The parameter a contains the information of the elastic modulus.

In order to accurately derive Young's modulus, the characteristics of the tip such as the tip radius, the cone angle and force constant should be carefully estimated [34–37]. Also, the tip deformation should be negligible. In the case of Si_3N_4 tips, the modulus of Young is 150 GPa [29,38] and for commercial silicon cantilevers Young's modulus is 169 GPa (according to the manufacturer).

The supporting sample – often glass substrates for biological objects – is crucial too, because it is often used as a reference sample appearing hard compared to the biomolecules. Glass itself is softer than the Si_3N_4 tip with a Young's modulus of 50 GPa and a force constant of about 50 N/m [29].

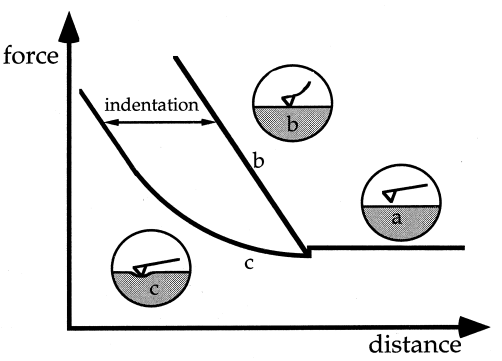

Fig. 1. Schematic representation of typical approach force-versus-distance curves on a hard (b) and a soft sample (c). The picture (a) shows the situation with no contact between tip and sample and in (b) a hard sample results in a deflection of the cantilever. Picture (c) shows the deformation of the soft sample by the tip which results in deviation from the linear relationship between the force and the distance seen before. The difference in deflection between the two curves is a measure of the indentation.

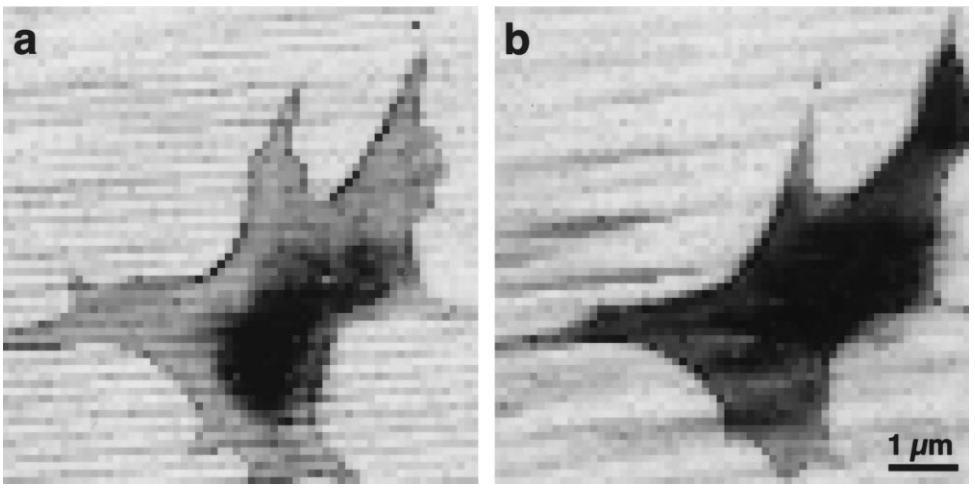

Fig. 2. FIEL maps of a living human platelet adsorbed on glass before (a) and after adding the pore-forming protein streptolysin O (b). In (b) a clear decrease in elasticity is observed. The black color represents a lower relative elasticity. Data provided by Walch et al. [48].

A hydrodynamic drag can occur due to the viscous effects of the surrounding liquid [39–41], which adds a constant external force to the loading force of the cantilever[1]. External vibrations or thermic vibrations of the cantilever usually will not really change the force measurements because the amplitude resulting from them is less than 0.1 nm [42].

Still, many assumptions have been made for an accurate determination of the elastic modulus. The sample, which is assumed to be an isotropic, smooth, elastic substrate, is, however, usually anisotropic and rough. The molecular roughness of the tip, the uncertainty of the contact area and a small lateral component in the applied force due to the approach with a small angle are usually ignored and will influence the accuracy of the measurement.

In fact, the absolute determination of Young's modulus of all biological system, which is complex, is not always necessary. Very often only a comparison between two different states are needed. In this case, the FIEL (force integration to equal limits) mapping, described by A-Hassan et al. [43], allows the acquisition of elastic data without worrying about some of the parameters described above. Individual force curves can be interpreted into arrays of relative elastic values, which can be related to a topographic image. This kind of 'elastic mapping' can provide valuable insight into the biological importance of e.g. cellular mechanics and their regulation.

[1] Due to the viscosity of the liquid, the hydrodynamic drag can be seen as a separation of the off-surface parts of the approaching and retracting force curves, which adds a constant external force to the loading force of the cantilever. The higher the scan velocity, the more the approach and retract curves are separated. A linear relationship between the separation of the approach and retract curves and the scan velocity has been observed. The hydrodynamic drag has an effect on the results when a comparison is made between the approach and the retract parts of the force curves (off surface). It is less so, but still important when only the center portion of one trace is evaluated. To deal with this force offset in the analysis, the force curves obtained during approach and retract can be averaged.

4. Examples of biological applications

4.1. Cells and organelles

A lot of effort has gone into the area of cells in order to obtain a better understanding of their mechanical properties by AFM. The elastic response of the cell is mainly due to its cytoskeleton which consists of a network of actin, microtubules, intermediate filaments and associated proteins [11,44].

Weisenhorn et al. [29] (living cell) were the first to quantify the elastic behavior of cells from force curves and obtained a Young's modulus of 0.013–0.15 MPa for a living (lung carcinoma) cell. Radmacher et al. then applied force spectroscopy to quantify the elastic modulus at different locations, i.e. of different organelles of human platelets: Young's moduli ranged from 1 to 50 kPa (Hertz' model) [41]. A sizeable discrepancy was observed between the experimental data and simulations on the basis of Hertz' model. Yet, the correlation observed between the position on the platelet and the changing elastic modulus is an interesting observation, which was shown to be related to the underlying cytoskeleton. Micromechanical measurements performed on cultured rat atrial myocytes showed a similar dependence of the elastic modulus on the position on the cell [45]. Young's modulus in a nuclear region of the cell was 0.5–0.67 MPa (Ca^{2+}-free solution, Sneddon mechanics), and increased 5–8-fold toward the periphery. These variations in stiffness could be related to the cytoskeletal heterogeneity (combining AFM and fluorescence imaging) [45] and did not, therefore, only depend on the height of the sample.

The regulation of the cytoskeletal filament assembly is influenced by the focal adhesion complex, where the protein vinculin can be found. Based on elasticity measurements, vinculin was shown to be a mechanical link between cell surface and cytoskeleton [46,47]. The elastic modulus for wild type and vinculin-deficient mouse F9 embryonic carcinoma cells is 3.8 kPa and 2.5 kPa, respectively (Hertz' model). A similar result has been found for the storage (elasticity) and loss modulus (viscosity) determined by rheology.

Dynamic changes in mechanical properties have also been observed [45]: increasing the calcium concentration (0 to 5 mM) lead to a $\sim$2-fold increase in the cell (myocyte) stiffness;

and a dynamic increase in cell stiffness also occurred during cell contraction, which is consistent with cross-bridge (actin-myosin) formation and force generation during contraction. FIEL maps (Fig. 2) showed that adding a pore-forming protein to the buffer solution also leads to a dynamic decrease in the elasticity of human platelets adsorbed on glass slides [48].

A very intriguing and interesting application is the construction of a sensor based on the detection of changes in the mechanical behavior of living cells using a thin cantilever [49]. Their preliminary data demonstrated that these cell sensors are capable of detecting the response of the cells to toxins. This sensor can provide a new way to study the mechanical behavior of living cells and their responses to effectors.

Elastic properties of cellular organelles can also be studied. Young's modulus of sub-micrometer-sized secretory granules isolated from rat mast cells ranged from 4.3 MPa (in La^{3+}) to 37 kPa (in $Na^{+)}$ with the value in Ca^{2+} in between (Hertz' model) [50]. A 10-fold increase in the matrix volume occurred. The elastic modulus showed a radial dependence which most likely originated from differences in the biochemical composition of the core (cross-linked proteoglycans) among the granule matrices. The matrix of secretory granules also seems to have the same mechanical properties as ion exchange gels. A swollen mast cell granule had an elastic modulus similar to gelatin in (pure) water which was 20 kPA (Hertz' model) [51]. Changing the fluid conditions (water/propanol ratio) induced changes in the elastic modulus for gelatin. Young's modulus increased to more than 0.1 GPa in pure propanol [51]. Thus, by changing the liquid environment the elastic modulus can be tuned, which is useful for improving the lateral resolution on biological samples. For example, depending on the buffer used (isoosmotic with and without calcium ions, and hypoosmotic buffer), the elastic modulus (Hertz' model) of a center of cholinergic synaptic vesicles from the electric organ of *Torpedo californica* ranged from 2 to 13×10^5 Pa [52].

4.2. Biomolecules: proteins and DNA

Another approach to better determine the elasticity of cells is the direct observation of the elasticity of the cytoskeletal proteins, such as microtubules (MTs) [33], even if for stability reasons they have to be fixed with glutaraldehyde in solution before immobilization onto the activated substrate. Increasing concentrations of glutaraldehyde showed an increasing stiffness of the MTs, consistent with what one would expect. From extrapolation to 0% glutaraldehyde, Young's modulus for MTs in vitro (in physiological solution) must be in the order of 3 MPa (Sneddon mechanics). The elastic modulus was only obtained from small indentations, because the underlying 'hard' silicon oxide sample can be felt by the tip at higher forces. Not only Young's modulus, but also a correct height determination of the MTs was obtained: the sum of the indentation and the average height at the same force always gave a value close to the true height (diameter) of the molecule [33]. This finding also explained the reduced height of unfixed chaperonin molecules – 4 ± 1 nm – under liquid [53].

Microtubules in air showed elastic behavior as long as the force applied was not too high. With imaging forces as high as 90 nN in air (contact mode AFM) their behavior was plastic (glutaraldehyde fixation of 0.1%) (A. Vinckier, unpublished results). The MT stayed deformed after imaging with lower forces. Higher concentrations of fixative (10% glutaraldehyde) led to no plastic behavior with forces even as high as 90 nN in air. On rehydrated chromosomes, a qualitative overview of the viscoelasticity with submicron resolution also has been obtained while applying various imaging forces [54].

Lysozyme adsorbed on mica, however, showed a high Young's modulus of 0.5 ± 0.2 GPa (Hertz' model) which is consistent with macroscopic measurements on wet crystals [40]. In the force curves obtained on lysozyme and on mica, a slowing down of the cantilever during liftoff is observed due to a viscous effect. On lysozyme an additional damping occurred, which gave an intrinsic viscosity for lysozyme of about 800 ± 400 Pa s. The theoretical considerations for the determination of the intrinsic viscosity is based on a damped harmonic oscillator [40].

The elasticity of the DNA duplex in the native and stretched states has been determined by direct measurements of the forces (i.e. force curves) applied to complementary DNA strands [55]. DNA, modeled as a uniform elastic rod, has an elastic modulus of 2.9×10^8 Pa for the native form and an increased elastic modulus of 2.0×10^9 Pa for the stretched state; thus the duplex became significantly stiffer after the structural transformation. Another possibility to obtain information about the mechanical properties of (bio)polymers like DNA is the determination of the persistence length from AFM images [56,57].

4.3. Elasticity measurements and lateral resolution in AFM imaging

The lateral resolution in AFM is limited by the elastic indentation [27,29,30,58,59]. Biological materials, such as cells, often show a lower lateral resolution which can be explained by their deformation due to the AFM tip [29]. When the tip indents a soft surface, a certain contact area between the tip and sample is created. This contact radius can be taken as a measure of the lateral resolution if one ignores the surface roughness [27]. From elastic experiments, Radmacher et al. [59] calculated a diameter between 500 and 50 nm for this contact area which is in a good agreement with the lateral resolution usually obtained on cells. Forces in the pN range (1–10 pN) are required to obtain high-resolution images on biological materials with about 1 nm vertical deformation and only a few nm^2 area of contact [29,30,60].

The imaging conditions of soft samples can be improved by increasing the elastic modulus of the sample, by reducing adhesive forces (e.g. capillary forces in air) and by reducing the applied force to a minimum.

5. Conclusion and outlook

AFM opens an additional possibility to obtain information about the mechanical properties, such as Young's modulus, of biological systems and soft samples on the microscopic scale. A major advantage of AFM over other methods is its lateral resolution which is of paramount importance at the μm and nm scale. It allows elastic data to be correlated with morphological ones. Local determination of the mechanical properties in combination with the topography will in the first place improve the understanding of the sample itself, but will also give a better insight into the mechanism and function of biosystems.

Improvements, such as better defined tips, a more precisely controllable force detection system, more elaborate theoretical

models, and a better knowledge of the tip-sample contact area and interactions, apart from other features, will contribute to more accurate measurements. These improvements will open the possibility to study the viscoelastic and plastic behavior of biological samples in more detail. Also, a better understanding of the mechanical properties in the nm dimension will lead to an improved, non-destructive, high-resolution imaging of e.g. cells.

Acknowledgements: We would like to thank J.A. DeRose, F. Zaugg, and U. Ziegler for useful discussions and careful reading of this minireview. We are also grateful to E. Ungewickell for providing us with clathrin cages. M. Walch is kindly acknowledged for Figure 2. This work was supported in part by the SNSF, Berne and the MURST, Rome.

References

[1] Binnig, G., Quate, C.F. and Gerber, C. (1986) Phys. Rev. Lett. 56, 930–933.
[2] Engel, A. (1991) Annu. Rev. Biophys. Biophys. Chem. 20, 79–108.
[3] Hansma, H.G. and Hoh, J.H. (1994) Annu. Rev. Biophys. Biomol. Struct. 23, 115–139.
[4] Shao, Z. and Yang, J. (1995) Q. Rev. Biophys. 28, 195–251.
[5] Lal, R. and John, S.A. (1994) Am. J. Physiol. 266, C1–21.
[6] Pethica, J.B. and Oliver, W.C. (1987) Phys. Scr. T 19, 61–66.
[7] Burnham, N. and Colton, R.J. (1989) J. Vac. Sci. Technol. A 7, 2906–2913.
[8] Maivald, P., Butt, H.-J., Gould, S.A.C., Prater, C.B., Drake, B., Gurley, J.A., Elings, V.B. and Hansma, P.K. (1991) Nanotechnology 2, 103–106.
[9] Tao, N.J., Lindsay, S.M. and Lees, S. (1992) Biophys. J. 63, 1165–1169.
[10] Ashkin, A. and Dziedzic, J.M. (1989) Proc. Natl. Acad. Sci. USA 86, 7914–7918.
[11] Janmey, P.A., Hvidt, S., Käs, J., Lerche, D., Maggs, A., Sackmann, E., Schliwa, M. and Stossel, T.P. (1994) J. Biol. Chem. 269, 32503–32513.
[12] Israelachvili, J. (1989) Intermolecular and Surface Forces, Academic Press, San Diego, CA.
[13] Evans, E., Ritchie, K. and Merkel, R. (1995) Biophys. J. 68, 2215–2216.
[14] Petersen, N.O., McConnaughey, W.B. and Elson, E.L. (1982) Proc. Natl. Acad. Sci. USA 79, 5327–5331.
[15] Hildebrand, J.A. and Rugar, D. (1984) J. Microsc. 134, 245–260.
[16] Zeman, K., Engelhard, H. and Sackmann, E. (1990) Eur. Biophys. J. 18, 203–219.
[17] Duquette, J.J., Grigg, P. and Hoffman, A.H. (1996) J. Biomech. Eng. 118, 557–564.
[18] Grazi, E., Magri, E., Schwienbacher, C. and Trombetta, G. (1996) FEBS Lett. 387, 101–104.
[19] Smith, C.W., Young, I.S. and Kearney, J.N. (1996) J. Biomech. Eng. 118, 56–61.
[20] Weisenhorn, A.L., Hansma, P.K., Albrecht, T.R. and Quate, C.F. (1989) Appl. Phys. Lett. 54, 2651–2653.
[21] Cappella, B., Baschieri, P., Frediani, C., Miccoli, P. and Ascoli, C. (1997) IEEE Eng. Med. Biol. 16, 58–65.
[22] Timoshenko, S.P. and Goodier, J.N. (1970) Theory of Elasticity, McGraw-Hill, London.
[23] Serway, R.A. (1982) pp. 298–301, Physics: for Scientists and Engineers CBS College Publishing, London.
[24] Hertz, H. (1881) J. Reine Angew. Math. 92, 156–171.
[25] Lur'e, A.I. (1964) in: Radok, J.R.M. (Ed.), Three-dimensional Problems of the Theory of Elasticity pp. 314–323, Interscience, London.
[26] Sneddon, I.N. (1965) Int. J. Eng. Sci. 3, 47–57.
[27] Heuberger, M., Dietler, G. and Schlapbach, L. (1994) Nanotechnology 5, 12–23.
[28] Weast, R.C. (1976), Handbook of Chemistry and Physics, Vol. F, Chemical Rubber Publishing Company, Boca Raton, FL.
[29] Weisenhorn, A.L., Khorsandi, M., Kasas, S., Gotzos, V. and Butt, H.-J. (1993) Nanotechnology 4, 106–113.
[30] Heuberger, M., Dietler, G. and Schlapbach, L. (1996) J. Vac. Sci. Technol. B 14, 1250–1254.
[31] Johnson, K.L., Kendall, K. and Roberts, A.D. (1971) Proc. R. Soc. Lond. Ser. A 324, 301–313.
[32] Landau, L.D. and Lifshitz, E.M. (1986) Statistical Physics Pergamon Press, Oxford.
[33] Vinckier, A., Dumortier, C., Engelborghs, Y. and Hellemans, L. (1996) J. Vac. Sci. Technol. B 14, 1427–1431.
[34] Albrecht, T.R., Akamine, S., Carver, T.E. and Quate, C.F. (1990) J. Vac. Sci. Technol. A 8, 3386–3396.
[35] Cleveland, J.P., Manne, S., Bocek, D. and Hansma, P.K. (1993) Rev. Sci. Instrum. 64, 403–405.
[36] Stokey, W.F. (1996) in: Shock and Vibration Handbook (Harris, C.M., Ed.), Ch. 7, McGraw-Hill, New York.
[37] DeRose, J.A. and Revel, J.-P. (1997) Microsc. Microanal. 3, 203–213.
[38] Grafström, S., Neitzert, M., Hagen, T., Ackermann, J., Neumann, R., Ptobst, O. and Wörtge, M. (1993) Nanotechnology 4, 143–151.
[39] Hoh, J. and Engel, A. (1993) Langmuir 9, 3310–3312.
[40] Radmacher, M., Fritz, M., Cleveland, J.P., Walters, D.A. and Hansma, P.K. (1994) Langmuir 10, 3809–3814.
[41] Radmacher, M., Fritz, M., Kacher, C.M., Cleveland, J.P. and Hansma, P.K. (1996) Biophys. J. 70, 556–567.
[42] Hansma, P.K., Elings, V.B., Marti, O. and Bracker, C.E. (1988) Science 242, 209–216.
[43] A-Hassan, E., Heinz, W.F., Antonik, M.D., D'Costa, N.P., Nageswaran, S., Schoenenberger, C.-A. and Hoh, J.H. (1998) Biophys. J. 74, 1564–1578.
[44] Stryer, L. (1988) W.H. Freeman and Company, New York.
[45] Shroff, S.G., Saner, D.R. and Lal, R. (1995) Am. J. Physiol. 269, C286–292.
[46] Goldmann, W.H. and Ezzell, R.M. (1996) Exp. Cell Res. 226, 234–237.
[47] Goldmann, W.H., Galneder, R., Ludwig, M., Kromm, A. and Ezzell, R.M. (1998) FEBS Lett. 424, 139–142.
[48] Walch, M., Ziegler, U. and Groscurth, P. (1998) to be published.
[49] Antonik, M.D., D'Costa, N.P. and Hoh, J.H. (1997) IEEE Eng. Med. Biol. 16, 66–72.
[50] Parpura, V. and Fernandez, J.M. (1996) Biophys. J. 71, 2356–2366.
[51] Radmacher, M., Fritz, M. and Hansma, P.K. (1995) Biophys. J. 69, 264–270.
[52] Laney, D.E., Garcia, R.A., Parsons, S.M. and Hansma, H.G. (1997) Biophys. J. 72, 806–813.
[53] Vinckier, A., Gervasoni, P., Zaugg, F., Ziegler, U., Lindner, P., Groscurth, P., Plückthun, A. and Semenza, G. (1998) Biophys. J. 74, 3256–3263.
[54] Fritzsche, W. and Henderson, E. (1997) Ultramicroscopy 69, 191–200.
[55] Noy, A., Vezenov, D.V., Kayyem, J.F., Meade, T.J. and Lieber, C.M. (1997) Chem. Biol. 4, 519–527.
[56] Rivetti, C., Guthold, M. and Bustamante, C. (1996) J. Mol. Biol. 264, 919–932.
[57] Hansma, H.G., Kim, K.J., Laney, D.E., Garcia, R.A., Argaman, M., Allen, M.J. and Parsons, S.M. (1997) J. Struct. Biol. 119, 99–108.
[58] Yang, J., Mou, J., Yuan, J.Y. and Shao, Z. (1996) J. Microsc. 182, 106–113.
[59] Radmacher, M. (1997) IEEE Eng. Med. Biol. Mag. 16, 47–57.
[60] Persson, B.N.J. (1987) Chem. Phys. Lett. 141, 366–368.
[61] Xu, W., Mulhern, P.J., Blackford, B.L., Jericho, M.H., Firtel, M. and Beveridge, T.J. (1996) J. Bacteriol. 178, 3106–3112.
[62] Rho, J.Y., Tsui, T.Y. and Pharr, G.M. (1997) Biomaterials 18, 1325–1330.